

Origin of pseudoelastic behavior in Ti–Mo-based alloys

L. C. Zhang, T. Zhou, S. P. Alpay, and M. Aindow^{a)}
*Department of Materials Science and Engineering, Institute of Materials Science,
 University of Connecticut, Storrs, Connecticut 06269-3136*

M. H. Wu
Memry Corporation, Bethel, Connecticut 06801

(Received 29 July 2005; accepted 13 October 2005; published online 7 December 2005)

High-resolution transmission electron microscopy and *in situ* x-ray diffraction analyses have been used to elucidate the compositional sensitivity of the deformation behavior in two β -Ti–Mo-based alloys. The alloy with 8% Mo exhibited conventional elastic/plastic behavior in tension which corresponds to the irreversible formation of stress-induced orthorhombic α'' martensite. The alloy with 10% Mo exhibited a pronounced pseudoelastic response with recovery of $\approx 80\%$ of the imposed tensile strain. This phenomenon is associated with the formation of another orthorhombic martensitic phase, which has not been reported previously, and this nucleates from pre-existing domains in the β matrix. © 2005 American Institute of Physics. [DOI: 10.1063/1.2142089]

Martensitic phase transformations are diffusionless, first-order, structural transitions in which the martensite phase is related to the initial phase by an invariant plane strain.^{1–3} Most martensitic phases form irreversibly due to the pinning of the interfaces by dislocations or other crystal defects. However, in certain Ni–Ti, Cu-, and Fe-based alloys,⁴ the martensite/matrix interfaces, and those between martensite variants, are highly mobile, giving rise to both the shape memory effect and pseudoelastic deformation behavior. In the latter case, deformation occurs by the formation of stress-induced martensite (SIM), which returns to the initial state spontaneously upon unloading.⁵ Pseudoelastic alloys are particularly attractive for a range of biomedical applications but concerns have been raised about the use of Ni–Ti *in vivo* because of the toxicity of Ni. More recently, a variety of biocompatible pseudoelastic metastable β -Ti alloys have been developed (e.g., Refs. 6 and 7) that display up to 80% strain recovery. There is, however, no clear understanding of the mechanism responsible for the pseudoelastic response in these alloys. This is mainly due to the complex microstructure of these materials compounded by inherent difficulties in the characterization of the reversible stress-induced deformation product(s). In this letter, we demonstrate that the pseudoelastic deformation in such alloys is due to the formation of a metastable orthorhombic martensitic phase, which has not been reported previously.

β -Ti alloys may transform to a wide variety of equilibrium and metastable phases upon cooling. Pure Ti undergoes an allotropic transformation at 833 °C from the high-temperature β phase, which is bcc with space group $Im\bar{3}m$ (No. 229), to the low-temperature hcp α phase ($P6_3/mmc$, No. 194). With the addition of β -stabilizing elements such as Mo, the transformation temperature decreases and the hcp phase can form by diffusion-controlled nucleation and growth, or by a diffusionless martensitic transformation wherein it is denoted α' . In alloys with higher levels of β -stabilizing additions, the β phase can be retained in a metastable form at RT upon rapid cooling from high temperatures (i.e., within the β phase field). Two further marten-

sitic phases can form in such alloys: ω and α'' (e.g., Ref. 8). The ω phase is a hexagonal derivative of the bcc structure with space group $P\bar{3}m1$ (No. 164), whereas the α'' phase exhibits an orthorhombic structure ($Cmcm$, No. 63) which corresponds to a distorted hcp lattice. Pseudoelasticity is usually attributed to the reversibility of a SIM but it is not clear which martensitic phase is responsible for this behavior in β -Ti alloys. For Ti–Mo-based alloys it is generally believed that it is the formation of the α'' phase which gives rise to the pseudoelasticity, but our recent deformation and x-ray diffraction (XRD) studies on a series of such alloys indicate that this is not the phase involved.⁶

Based upon our previous work,⁶ a series of six experimental Ti–Mo-based alloys were prepared by double vacuum-arc melting. These had compositions (in weight percent) of Ti– x Mo–4Nb–2V–3Al where $x=8–11$. The alloy buttons were hot rolled and solution treated at 870 °C in air, followed by air cooling. In order to promote pseudoelasticity, the materials were then flash annealed at 550 °C for 10 s.⁶ The tensile properties of the heat-treated samples were determined using an Instron model 5565 testing frame with appropriate extensometry. A custom-built straining stage was used to perform *in situ* x-ray analysis on a Bruker AXS D5005 diffractometer using Cu K_α radiation. High purity alumina powder was dispersed on the sample surface to give an accurate internal standard for calibration of the x-ray spectra. The deformation micromechanisms were investigated using transmission electron microscopy (TEM) to compare the structures before and after deformation. TEM data were obtained in a JEOL JEM-2010 UHR FasTEM operating at an accelerating voltage of 200 kV.

In previous work on β -Ti–Mo-based alloys we have shown that the pseudoelastic response is a sensitive function of composition, requiring Mo contents above a critical level of about 9%. Thus, for brevity we present here only data from the 8Mo and 10Mo alloys, corresponding to compositions below and above the critical Mo content for pseudoelasticity, respectively. Tensile stress/strain and *in situ* XRD data from these alloys are presented in Fig. 1. As expected, the 8Mo alloy does not exhibit any significant tensile pseudoelastic response [Fig. 1(a)]. A series of x-ray spectra

^{a)}Electronic mail: m.aindow@uconn.edu

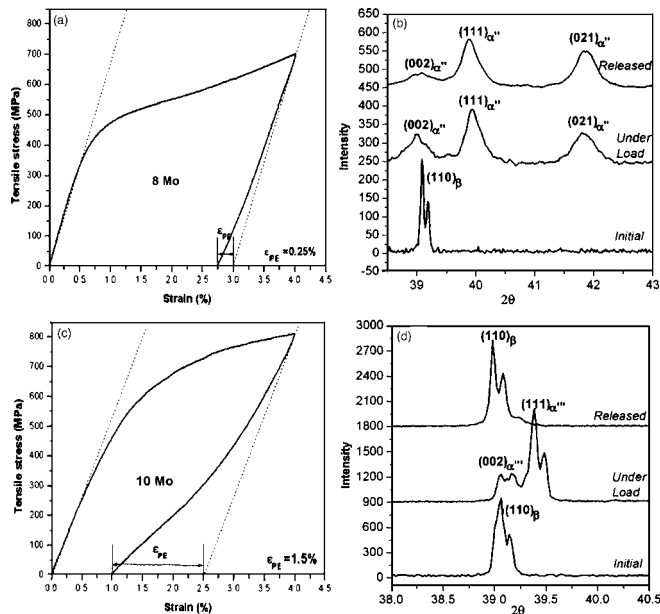


FIG. 1. Data obtained from the 8Mo (a), (b) and 10Mo (c), (d) alloys in uniaxial tension. (a) and (c) engineering stress-strain curves. (b) and (d) x-ray spectra obtained before straining, with a 4% imposed strain, and after unloading. The x-ray spectra have been smoothed, normalized and displaced along the Y axis for clarity. The strain in the *in situ* x-ray diffraction experiment was also estimated to be $\sim 4\%$.

corresponding to the unstressed, stressed ($\approx 4\%$ imposed strain) and stress-released states are shown in Fig. 1(b). These data confirm that, prior to straining, only the β phase with $a=0.320$ nm is present. We note, however, that the initial 110_{β} peak showed a very slight splitting of about 0.1° . Upon loading, pronounced martensitic peaks appeared and there was a concomitant reduction in the 110_{β} peak. The two major martensitic peaks at 39.0° and 39.9° , correspond exactly to those expected for 002 and 111 in the α' phase with $a=0.301$ nm, $b=0.491$ nm, and $c=0.463$ nm. No significant changes were observed upon unloading demonstrating that the stress-induced α' martensite is *irreversible* in this alloy. For the 10Mo alloy, however, a pronounced pseudoelastic tensile response was observed with $\sim 80\%$ of the imposed strain being recovered upon unloading [Fig. 1(c)]. Corresponding differences were observed in the *in situ* XRD data [Fig. 1(d)]. Here again martensitic peaks developed upon loading, but in this case the positions of these (39.1° and 39.4°) did not correspond to those expected for the α' phase. Moreover, upon unloading these martensitic peaks disappeared from the x-ray spectrum leaving only the 110_{β} peak. While these data confirm that the pseudoelastic response in the 10Mo alloy is due to the formation of a reversible SIM, they demonstrate unequivocally that this martensite is not the α' phase (or indeed any other known phase in this system).

The character of the martensitic phases was investigated using high-resolution TEM (HRTEM). A typical HRTEM image obtained from the interface between a SIM lath and the β matrix in the deformed 8Mo alloy is shown in Fig. 2(a). The inset is a fast Fourier transform (FFT) of the martensite side of the image showing that this corresponds to an $[001]$ zone axis lattice image for the α' phase. Both the habit plane and the orientation relationship between the α' martensite and the β matrix are consistent with those observed in our recent work on nucleation of stress-induced α' martensite.⁹

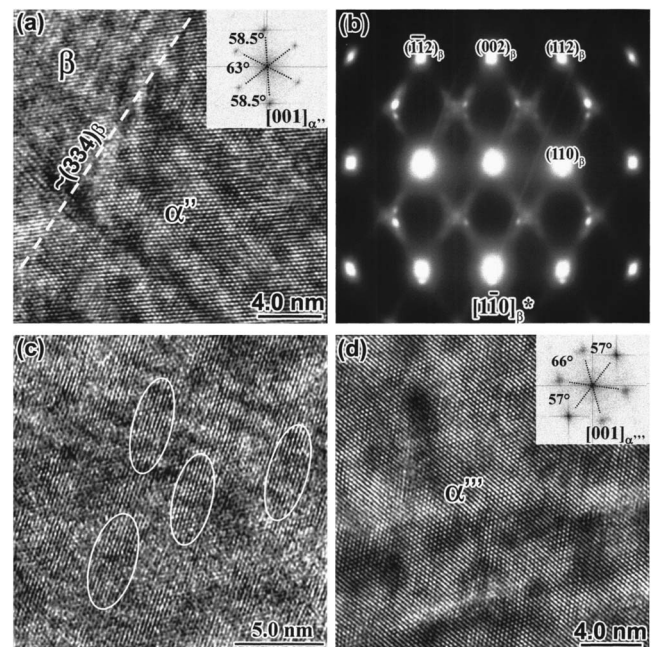


FIG. 2. Structural characteristics of the alloys: (a) HRTEM image obtained from an α' SIM/ β interface in the deformed 8Mo sample at the $[001]_{\alpha'}$ zone axis, with the FFT from the α' region inset; (b) and (c) selected area electron diffraction pattern and HRTEM image, respectively, obtained from the undeformed 10Mo sample at the $[1\bar{1}0]_{\beta}$ zone axis; (d) HRTEM image (with inset FFT) obtained from the deformed 10Mo sample at the $[001]$ zone axis of the SIM retained at the boundary with a $\{332\}$ twin.

The analysis of the SIM in the 10Mo alloy is much more challenging since this is a *reversible* martensite and, as such, the phase of interest is essentially eliminated from the deformation microstructure upon unloading. Figures 2(b) and 2(c) are typical examples of electron diffraction patterns and HRTEM images obtained from the *undeformed* 10Mo alloy at the $[1\bar{1}0]_{\beta}$ zone axis. In addition to the main diffraction spots from the β matrix, the diffraction pattern contains streaks lying parallel to the 112-type scattering vectors and additional weak diffraction spots clustered around the $1/2\{112\}_{\beta}$ positions. Streaking along 112-type directions has been observed for other metastable β -Ti-based alloys after quenching or low-temperature aging (e.g., Ref. 10), and this corresponds to “diffuse ω ” ordering. The configuration of the additional weak diffraction spots resembles the $[001]$ zone axis pattern for the α' phase, but a more careful analysis shows that the angles and spacings do not correspond exactly to those for this phase. By using high-pass FFT filtering of HRTEM images it was shown that the weak diffraction spots arise from small ellipsoidal domains ≈ 2 nm across and ≈ 5 nm in length; four examples of these are indicated in Fig. 2(c). We note that no such domains were observed in the 8Mo alloy and infer that the domains correspond to the nuclei from which the new reversible martensite forms. It was, however, not possible to determine the structure of this martensite directly due to the interference from coherent strain field in the β -matrix.

Although the reversible SIM is essentially eliminated from the microstructure during the unloading, occasional paths of this phase were retained at the boundaries with $\{332\}$ twins. These unusual twins have been observed previously in Ti–Mo-based alloys¹¹ and it is now accepted that their formation is associated with a transition through an intermedi-

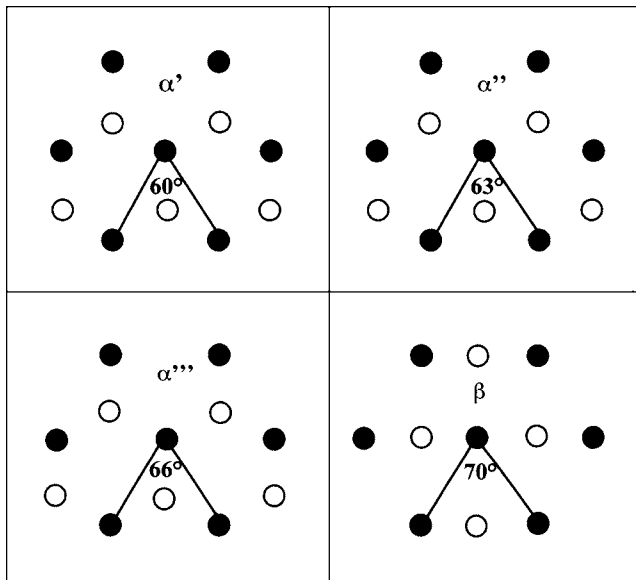


FIG. 3. Schematic projections showing the relationship between the crystal structures of the martensites and the β matrix: α' along $[0001]$; α'' along $[001]$; α''' along $[001]$ and β structure viewed along $\langle 110 \rangle$, respectively. Symbols \bullet and \circ represent atoms in the projection plane and in the layers above and below the projection plane, respectively.

ate martensitic state.^{12,13} A detailed discussion on the origins of these $\{332\}$ twins will be presented elsewhere but we infer that the twin formation pins the martensite, preventing the reverse transformation and enabling the structure to be revealed directly. Figure 2(d) is one of the few clear examples we have obtained of HRTEM images from the SIM structure in the unloaded sample, and the corresponding FFT is inset. The lattice image and FFT are similar to those in $[001]$ HRTEM images from the α'' phase, but in this case the included angle between the 110-type reflections is 66° , not 70° . These data suggest that the reversible SIM phase has the same orthorhombic symmetry as the α'' phase ($Cmcm$, No. 63) but with lattice parameters $a=0.3067$ nm, $b=0.4723$ nm, and $c=0.4520$ nm. We note that the martensitic peaks observed in the *in situ* XRD spectra from the 10Mo alloy, and indeed the additional weak reflections in the electron diffraction patterns from undeformed samples of this alloy, are entirely consistent with these structural parameters.

Schematic projections of the three different martensitic structures are shown in Fig. 3 together with the corresponding projection of the β -matrix structure. It is clear from these projections that the martensites can be considered as intermediate states in a structural transition from the bcc β struc-

ture to the hcp α' structure. Moreover, since the reversible SIM structure lies between that of the α'' and β phases, the logical designation for this structure is α''' . One can use the magnitudes of the principal strains involved as a measure of the energy required to produce these three martensites from the β phase. If we define $\varepsilon_1=0$ perpendicular to the invariant plane, then $\varepsilon_2=-\varepsilon_3$ and: for $\beta \rightarrow \alpha'$, $\varepsilon_2=0.10$; for $\beta \rightarrow \alpha''$, $\varepsilon_2=0.07$; and for $\beta \rightarrow \alpha'''$, $\varepsilon_2=0.04$. This implies that the strain energy required to produce the martensitic transformation from β to α''' (and *vice versa*) would be much lower than that for the other martensites. Moreover, since this would correspond to the propagation of this transformation at a lower *stress*, the probability of generating lattice dislocations, which might pin the martensite boundaries, is greatly reduced. As such, one would expect not only that the α''' phase would form in preference to α'' , but also that this would be inherently more reversible.

In summary we have shown that the transition from elastic/plastic to pseudoelastic deformation in metastable β -Ti–Mo-based alloys corresponds to a transition in the SIM phase from the well-known α'' phase to a new orthorhombic α''' phase. This α''' phase grows from premartensitic domains in the initial β phase and is inherently more reversible than the α'' phase, because of the lower strain energy required to propagate the transformation.

The authors are very grateful to the late Professor Martin J. Blackburn who inspired them to pursue this work. Professor Blackburn died on March 12, 2004. Financial support was provided by Connecticut Innovations Incorporated and Memry Corporation.

¹G. R. Barsch and J. A. Krumhansl, Phys. Rev. Lett. **53**, 1069 (1984).

²A. E. Jacobs, Phys. Rev. B **31**, 5984 (1985).

³G. L. Krasko and G. B. Olson, Phys. Rev. B **40**, 11536 (1989).

⁴See for example: M. A. M. Bourke, R. Vaidyanathan, and D. C. Dunand, Appl. Phys. Lett. **69**, 2477 (1996); F. F. Gong, H. M. Shen, and Y. N. Wang, *ibid.* **69**, 2656 (1996); J. Marcos, A. Planes, and L. Manosa, Phys. Rev. B **66**, 054428 (2002).

⁵A. L. Roytburd and J. Slutsker, J. Appl. Phys. **77**, 2745 (1995).

⁶T. Zhou, M. Aindow, S. P. Alpay, M. J. Blackburn, and M. H. Wu, Scr. Mater. **50**, 343 (2004).

⁷E. Takahashi, T. Sakurai, S. Watanabe, N. Masahashi, and S. Hanada, Mater. Trans., JIM **43**, 2978 (2002).

⁸A. Ramesh and S. Ankem, Metall. Mater. Trans. A **30**, 2249 (1999).

⁹L. C. Zhang, T. Zhou, M. Aindow, S. P. Alpay, M. J. Blackburn, and M. H. Wu, J. Mater. Sci. **40**, 2833 (2005).

¹⁰K. K. McCabe and S. L. Sass, Philos. Mag. **23**, 957 (1971).

¹¹M. J. Blackburn and J. A. Feeney, J. Inst. Met. **99**, 132 (1971).

¹²Y. Takemoto, M. Hida, and A. Sakakibara, J. Jpn. Inst. Met. **60**, 1072 (1996).

¹³Y. R. Nemirovskii, Phys. Met. Metallogr. **86**, 20 (1998).